

# Tailoring RF Power Distribution for Body Torso MRI at 300MHz

J. Tian<sup>1</sup>, A. Gopinath<sup>2</sup>, and J. T. Vaughan<sup>2</sup>

<sup>1</sup>Center for Magnetic Resonance Research, University of Minnesota, Minneapolis, Minnesota, United States, <sup>2</sup>University of Minnesota

## Introduction

Simulation and image experiments showed problems existed in 7T body torso imaging, including  $B_1^+$ /imaging in-homogeneity including the longitudinal lines with significant artifacts, and low  $|B_1^+|$ /Power in the body torso due to high RF radiation loss and the undesired RF energy dissipation in the rest of the body (1,2). The low-efficiency transmission produces low SNR, and thus does not show the advantages of high frequency MRI.

To solve the problems, waveguides were modified to tailor the RF power distribution with antennas (3,4). These measures are not the appropriate solutions to body MRI with TEM coils, which has high  $|B_1^+|$ /Power and lower SAR (5). Metals close to human body may also raise RF safety concerns. 2~4 cm thin dielectric pads had been used at 3T body abdominal and 7T head scans successfully in improving  $B_1^+$  homogeneity and magnitude in the imaging ROI (6-8).

In this abstract, we propose three dielectric methods to modulate the RF power distribution within human body and to improve the  $|B_1^+|$ /Power accordingly in the torso. These dielectric methods were evaluated quantitatively with the RF wave theory, and verified by electromagnetic simulations.

## Theory

1). For norm incidence, if a  $\lambda/4$  dielectric pad (intrinsic impedance  $Z_3$ ) is inserted between air and the body, then no reflection occurs when  $Z_3$  equals to  $\sqrt{Z_1 Z_2}$  where  $Z_1$  is the intrinsic impedance for air, and  $Z_2$  is the input impedance looking into skin at the air/pad boundary. For oblique incidence of the RF waves of parallel polarization, a  $\lambda/4$  pads has minimum reflection at  $\epsilon_r=10$ , at which only about 30% or less of the incident RF power was reflected back at the air-pad boundary when incident angle  $\alpha_i \leq 45^\circ$ . Without the  $\lambda/4$  dielectric pad, over 82% of the incident RF power would be reflected back for the same incident angles (Figure 1). 2). 4cm thin layers of dielectric pads with different  $\epsilon_r$  were assessed with the RF oblique incidence theory. Minimum reflection is achieved with  $\epsilon_r=20$  for the 4cm thickness dielectric pad. 3). Power analysis with a body-size TEM coil suggests the major RF power dissipated in the head is from the active elements through the air around neck. To block the RF energy flowing out of the ROI, 2.5cm-thick dielectric boards with  $\epsilon_r=80$  is proposed at the ends of the TEM active elements. The angle of incident  $\alpha_i$  at the surface of the upper dielectric board ranges from  $30^\circ \sim 60^\circ$  for the RF waves propagating to the head. Theoretical estimation shows that for the RF waves of parallel polarization at least 90% of the incident RF energy would be reflected back into the ROI at the surface of the dielectric board for  $\alpha_i=30^\circ \sim 60^\circ$ .

## Methods

A body TEM array (16-ch, length:33cm, co-axial elements, id 57.5 cm, od 62.5cm) was used the FDTD simulation. The gradient (id: 67.5cm, od: 89cm, length: 125cm) and the magnetic bore (id: 90cm; length: 300cm) were included in simulation. The  $\lambda/4$  dielectric pad, thin dielectric pad, and the dielectric boards were then added separately to the original simulation. The  $\lambda/4$  pad ( $\epsilon_r=10$ ), located on the front and back of human torso in cylinder shape (od:44cm), was placed closely around the human torso. The 4cm thin dielectric pad ( $\epsilon_r=20$ ) was 6cm wide. The dielectric boards with  $\epsilon_r=80$  were 2.5cm in thickness and put around the neck. Steady state calculations were performed to calculate the fields and RF power distribution.

In the post-processing with Matlab, the  $|B_1^+|$  and the power distribution (P) over the central sagittal, coronal and transverse slices were calculated, and the total power was normalized to 1 Watt. The mean  $|B_1^+|$  averaged within the heart ( $B_{1H}$ ) and within all the body tissues ( $B_{1B}$ ) on the transverse slices and their ratios were computed.

## Results and Conclusions

The RF power distribution was present in Fig. 2, together with the statistics in Table 2, in which the ROI were the region between the two horizontal lines in the figure.

1). The  $\lambda/4$  pad minimizes the RF reflection, resulting in a higher percentage of power deposition with the ROI, and as a side effect reducing the radiation loss and the power dissipation in the rest of the body. It reduces the destructive RF phase interference within the heart, resulting in high  $B_1^+$  homogeneity with a high  $B_{1H}/B_{1B}$  ratio.

2). The 4cm pad has little effect in redistributing the RF power, lower than the theoretical prediction, mainly due to the fact that the 4cm dielectric pad covers only a small portion of the body. The  $B_{1H}/B_{1B}$  increase is a result of the reduced RF phase interferences in the torso, especially within the heart.

3). The dielectric board boosts the  $|B_1^+|$  globally within the ROI by reflecting the outgoing RF power back in the region. It does not help to moderate the RF in-homogeneity with the torso, or to improve  $|B_1^+|$  within a specific region in the torso, which is indicated by the relative ratios of  $B_{1H}/B_{1B}$  (Table 1): 48.19% for the original coil, and 49.44% for the coil+boards. Meanwhile the ratio is around 85% with the  $\lambda/4$  pad, and over 91% with the presence of the 4cm pad.

In summary, the numerical results agree with the theoretical analysis. All dielectric methods help improve the RF transmission efficiency.

**Acknowledgements:** NIH-NIBIB-EB000895, NIH-NIBIB-EB006835, NIH-NIBIB-EB007327, NIH-NCRR-P41-RR08079, P41- RR008079.

## References

1. Vaughan JT, et. MRM 61:244-248.
2. Zhang B, et. ISMRM 2009:499.
3. Mueller M, et. ISMRM 2010.
4. Adreychenko A, et. ISMRM 2010
5. Zhang B, et. ISMRM 2010.
6. Schmitt M, et. ISMRM 2004: 197.
7. Sreenivas M, et. Euro. J. of Rad. 62: 143-146.
8. Yang Q, et. JMRI 24: 197-202.

Table 1. Mean  $|B_1^+|$  on the central transverse slice for different simulation setup

Mean $ B_1^+ $	Original Coil	Plus $\lambda/4$ pad	Plus 4cm pad	Plus boards	Plus $\lambda/4$ pad and board	Plus 4cm pad and board
$B_{1H}$ ( $\mu T$ )	0.0320	0.0898	0.0660	0.0620	0.1128	0.1319
$B_{1B}$ ( $\mu T$ )	0.0664	0.1063	0.0723	0.1254	0.1316	0.1285
$B_{1H}/B_{1B}$	48.19%	84.48%	91.29	49.44%	85.71%	102.65%

Table 2. RF Power distributions for different simulation setup

Region	Original Coil	Plus $\lambda/4$ pad	Plus 4cm pad	Plus board	Plus $\lambda/4$ pad and board	Plus 4cm pad and board
Within ROI	36.91%	61.86%	39.58%	92.96%	93.54%	93.80%
Above ROI	4.94%	2.51%	3.99%	1.74%	1.78%	3.95%
Below ROI	37.60%	24.42%	36.27%	4.35%	4.39%	1.57%
Radiation	20.55%	11.21%	20.16%	0.95%	0.29%	0.69%

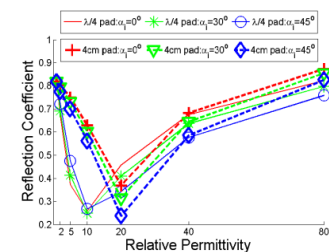


Figure 1.  $|T|$  vs.  $\epsilon_r$  for the  $\lambda/4$ , 4cm dielectric pads

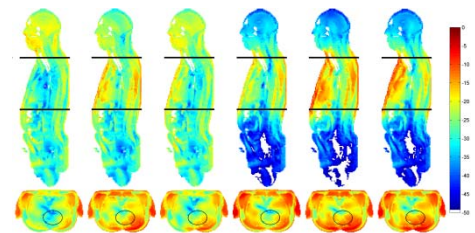


Figure 2. RF Power distribution, in the same order as appeared in the Tables, with heart outlined in the transverse slices